iScience

Article

# Regulation of Xvelo assembly by centrosomal proteins

## Graphical abstract

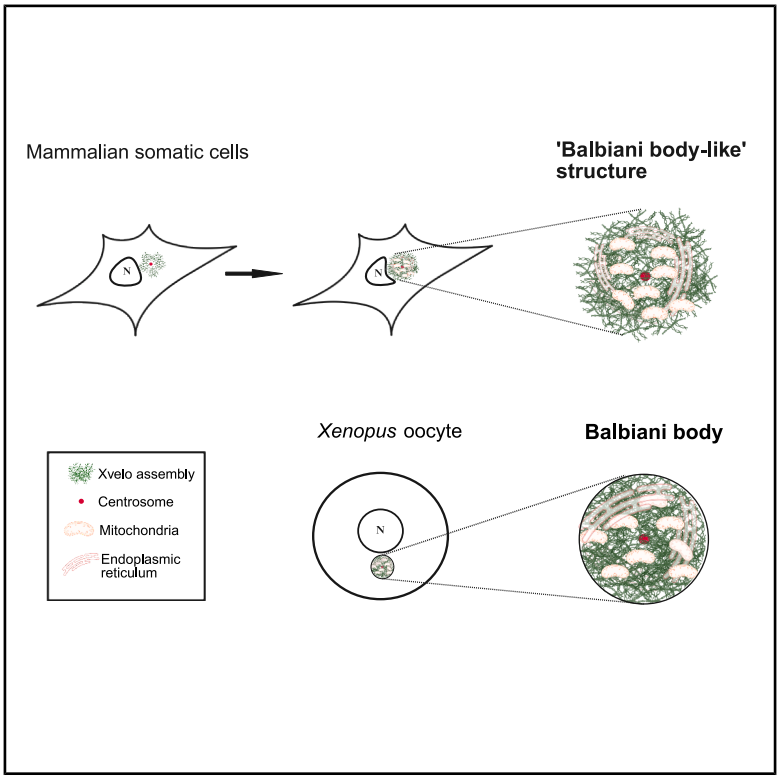


## Authors

Divyanshi, Meining Li, Elvan Böke, Jing Yang

## Correspondence

yangj@illinois.edu

## In brief

Biochemistry; Molecular biology; Cell biology

## Highlights

- Xvelo can assemble into a "Balbiani body-like" structure in mammalian somatic cells
- This "Balbiani body-like" structure shares key features of the oocyte Balbiani body
- Centrosome proteins directly interact with Xvelo and facilitate Xvelo assembly

Divyanshi et al., 2025, iScience *28*, 113805
November 21, 2025 
https://doi.org/10.1016/j.isci.2025.113805

CellPress

iScience

CellPress
OPEN ACCESS

Article

# Regulation of Xvelo assembly by centrosomal proteins

Divyanshi,[1] Meining Li,[2,5] Elvan Böke,[3,4] and Jing Yang[1,2,6,*]
[1]Department of Cell and Developmental Biology, University of Illinois at Urbana-Champaign, Champaign IL 61801, USA
[2]Department of Comparative Biosciences, University of Illinois at Urbana-Champaign, Champaign, IL 61802, USA
[3]Centre for Genomic Regulation (CRG), The Barcelona Institute of Science and Technology, 08003 Barcelona, Spain
[4]Institució Catalana de Recerca i Estudis Avançats (ICREA), 08010 Barcelona, Spain
[5]Present address: Department of Biochemistry & Molecular Biology, Shanxi Medical University, Taiyuan 030001, China
[6]Lead contact
*Correspondence: yangj@illinois.edu
https://doi.org/10.1016/j.isci.2025.113805

## SUMMARY

The oocyte Balbiani body (Bb) is a conserved membraneless organelle required for germline specification in many species. Here we report that when overexpressed in mammalian somatic cells, *Xenopus* Velo (Xvelo), the Bb matrix protein could reconstitute a "Bb-like" structure, which shares key features of the oocyte Bb. Using this system, we investigated the potential mechanism of Bb assembly. We focused on the involvement of centrosomal proteins in this process, as both endogenous oocyte Bb and the "Bb-like" structure induced by Xvelo overexpression form around the centrosome. Our results reveal that multiple components of the centrosome can interact with Xvelo and promote Xvelo assembly to varying degrees. Moreover, knockdown of these proteins reduces Xvelo assembly. Our findings thus suggest that the interaction between centrosomal proteins and Xvelo may facilitate the initial aggregation of Xvelo, leading to the assembly of Bb around the centrosome in the oocyte.

## INTRODUCTION

Recent works have highlighted the fundamental roles of membraneless biomolecular condensates in a wide variety of biological processes.[1–3] By enriching biomolecules in specific subcellular compartments, membraneless condensates can either facilitate biochemical reactions inside the cell or regulate the half-life of their cargoes. Increasing evidence has demonstrated that under physiological conditions, membraneless condensates are involved in gene regulation at transcriptional, translational, and post-translational levels.[4–7] However, the formation of pathological condensates can be toxic to the cell, leading to devastating conditions such as neurodegenerative diseases in humans.[8,9]

Membraneless condensates are fundamental for germline development.[10,11] Several condensates unique to the germline have been identified across different species, such as the P granules or germline P bodies in the worm,[12] polar granules in the fly,[10,13] L body in the frog,[14,15] and male (XY) sex body in mammals.[16–18] Apart from these dynamic gel/liquid-like condensates, stable amyloid-like protein assemblies also exist in the germline. Unlike pathological amyloids that accumulate under disease conditions,[8,9] these amyloid-like aggregates form under physiological conditions. In yeast, dynamic regulation of such condensates is essential for gametogenesis.[19,20] The Balbiani body (Bb), an amyloid-like condensate, first discovered more than a hundred years ago,[21,22] has been observed in the oocytes in many species.[10,23–25]

The Bb has been studied by several generations of researchers.[22,24,26,27] Studies in the 1800s first identified it as a granulofibrillar material in the oocytes of spiders.[21] It was later observed in *Drosophila*, *Xenopus*, zebrafish, mice, and human oocytes.[28–33] The conservation of this structure in oocytes through the course of evolution hints at its potential importance. Although the precise arrangement varies across species, the Bb houses abundant mitochondria, endoplasmic reticulum (ER), Golgi apparatus, and/or a specific set of proteins/RNAs.[22,28,29,34,35] It may play a role in ensuring the inheritance of healthy organelles by the next generation, which could explain the need for its conservation across species.[36–38] In *Xenopus* and zebrafish, the Bb accumulates the RNAs and proteins needed to specify future primordial germ cells (PGCs).[33,39–42] *Xenopus* Velo (Xvelo) and zebrafish Buckyball (Buc) proteins form the matrix for the Bb in these species.[30,33,39,42,43] In zebrafish Buc-null mutants, Bb cannot assemble in the oocyte. The mitochondria, ER, and germline determinants are dispersed in the entire cytoplasm. Likely due to defective animal-vegetal axis, embryos derived from *buc*$^{-/-}$ oocytes cannot form the blastodisc and die shortly after fertilization.[30,33,44]

The Xvelo protein contains an N-terminal prion-like domain (PLD) and a C-terminal intrinsically disordered region (IDR).[39,45] In general, proteins with IDRs or PLDs have a high propensity to take part in the process of phase separation.[1,39,45–49] It has been reported that the N-terminal PLD of Xvelo, which confers Xvelo the ability to self-assemble, is required for its localization

to the Bb in *Xenopus* oocytes. The efficient recruitment of RNA and organelles into the Bb, however, also requires the C-terminus of the protein.[39] While the Xvelo/Buc protein can self-assemble into an amyloid-like network *in vitro*[39] and is required for Bb formation in the oocyte,[30,33,44] it is currently unclear whether Xvelo/Buc alone can assemble into a Bb in the absence of other oocyte-specific factors. Although Bb assembly has started to gain attention recently,[50] the mechanism responsible for the initiation of this assembly during early oogenesis remains largely unknown.

In *Xenopus* and zebrafish, the Bb assembles around the centrosome in stage I oocytes.[51,52] The centrosome is a microtubule organizing center (MTOC) in the cell and consists of a pair of centrioles surrounded by the pericentriolar matrix (PCM).[53,54] In most species, centrioles are eliminated from the oocyte during later stages of oogenesis and are reintroduced by the sperm upon fertilization.[55–58] The centrosome is composed of hundreds of proteins. Many of these proteins have been studied during early development. For instance, polo-like kinase 4 (PLK4), which can partake in self-assembly via phase separation,[59,60] was shown to play an important role in the regulation of centriole duplication during early zebrafish embryogenesis.[61] The outer dense fiber isoform 9, also called cenexin, was recently reported to play a role in maintaining the integrity of the PCM in zebrafish embryos.[62] Perturbations to some centrosome proteins have also been shown to cause defects in the germline. Zebrafish embryos mutant for spindle assembly defective protein 6 (Sas6), which acts as the scaffold for the centrioles,[63–65] showed defective germ plasm recruitment to the cleavage furrows in early embryos.[66] Dzip1 is another component of the appendages at the mother centrioles with documented roles in both germline and somatic development. In somatic tissues, Dzip1 regulates ciliogenesis and is essential for the Hedgehog signaling in early embryos.[67–74] Dzip1 is dynamically expressed in vertebrate germline. It localizes to the Bb in *Xenopus* and zebrafish oocytes. Knockdown of Dzip1 impairs the development of *Xenopus* PGCs.[75] So far, whether Dzip1 or any other centrosomal proteins play a role in Bb assembly remains unknown.

In this study, we aimed to determine whether Xvelo protein has an intrinsic ability to assemble into a biomolecular condensate capable of recruiting components of the Bb and whether the centrosome plays a direct role in promoting the assembly of Xvelo into such a condensate. In the oocyte, the Bb contains Xvelo along with many other germline factors. To avoid detecting indirect mechanisms, we conducted our investigation in mammalian somatic cells, which lack any germ plasm components and oocyte-specific factors. Our findings reveal that Xvelo possesses the ability to assemble into a Bb-like structure around the centrosome in mammalian somatic cells. These Xvelo assemblies accumulate mitochondria and ER and can selectively enrich co-expressed germline proteins. Furthermore, we show that centrosomal proteins such as Sas6, cenexin, and DZIP1 are required for Xvelo assembly in mammalian somatic cells. These proteins directly interact with Xvelo and enhance its assembly around the centrosome, independent of oocyte-specific factors. Together, our results support the idea that assembly of Xvelo, aided by interactions with centrosome components, could initiate Bb formation around the centrosome, providing mechanistic insights into the initial steps of Bb formation.

## RESULTS

### Overexpression of Xvelo induces a "Bb-like" structure in mammalian somatic cells

The Bb assembles around the centrosome in early-stage oocytes.[51,52] In *Xenopus*, Xvelo protein forms the stable matrix of the Bb and was reported to show minimal recovery of fluorescence post photobleaching.[39] We found that when GFP-Xvelo was expressed in HEK293T cells, Xvelo in some cells assembled into aggregates (Figure 1A). The assembly of Xvelo aggregates is dose-dependent. At the conditions used for the majority of experiments in this study (0.5 μg plasmid per transfection), around 10% of Xvelo-expressing cells formed Xvelo aggregates and the rest showed an unlocalized Xvelo expression pattern (Figures 1A and 1B). To assess Xvelo assembly more quantitatively, we performed a fractionation experiment in which Xvelo-expressing cells were lysed with the NP40-containing lysis buffer, followed by centrifugation to separate the soluble (unlocalized Xvelo) and insoluble (Xvelo aggregates) protein (Figure 1C). The expression level of insoluble Xvelo was undetectable in cells transfected with 0.25 μg Xvelo expression construct. However, in cells transfected with 1 μg and 1.5 μg Xvelo plasmid, we found that around half of Xvelo was in the insoluble form (Figure 1C). In these transient transfection experiments, Xvelo assembles into aggregates over time, before eventually being degraded (Figure 1D). The Xvelo assemblies were resistant to digitonin extraction. This is in stark contrast to the GFP protein in the cytoplasm, which was extracted completely upon digitonin permeabilization of the cell (Figure 1E).

Strikingly, Xvelo often assembles in a perinuclear region, resembling the Bb in the oocyte, which forms around the centrosome.[52] To determine if the Xvelo aggregates form around the centrosome, we co-expressed Xvelo with centrosome proteins, mCherry-DZIP1[67] and RFP-HYLS[76] (Figure 1F). Indeed, we found that Xvelo always assembled around the centrosome in HEK293T cells, as seen by Xvelo assembly around the DZIP1/HYLS core. Previous fluorescence recovery after photobleaching (FRAP) experiments have demonstrated that in *Xenopus* and zebrafish, Xvelo/Buc protein forms a stable matrix for the Bb.[39,50] We thus performed a FRAP assay to test if these Xvelo assemblies had similar properties. We found that these Xvelo aggregates, like the Xvelo in oocyte Bb, recovered poorly after photobleaching (Figure 1G).

Inspired by the aforementioned findings, we further characterized the Xvelo assembly. It is well known that Bb accumulates organelles such as mitochondria and ER, and sequesters the germ plasm components.[22,24,26] In fact, the Bb was occasionally referred to as the mitochondrial cloud in *Xenopus*.[77] We thus tested if the Xvelo assemblies in HEK293T cells had the ability to recruit mitochondria, ER, and germ plasm components. In un-transfected cells, the mitochondria and ER are spread throughout the cell. In the cells with Xvelo assembly, however, the mitochondria and ER are selectively enriched into the Xvelo assembly (Figures 2A and 2B). Thus, overexpression of the Xvelo protein alone was sufficient for reconstituting a "Bb-like"

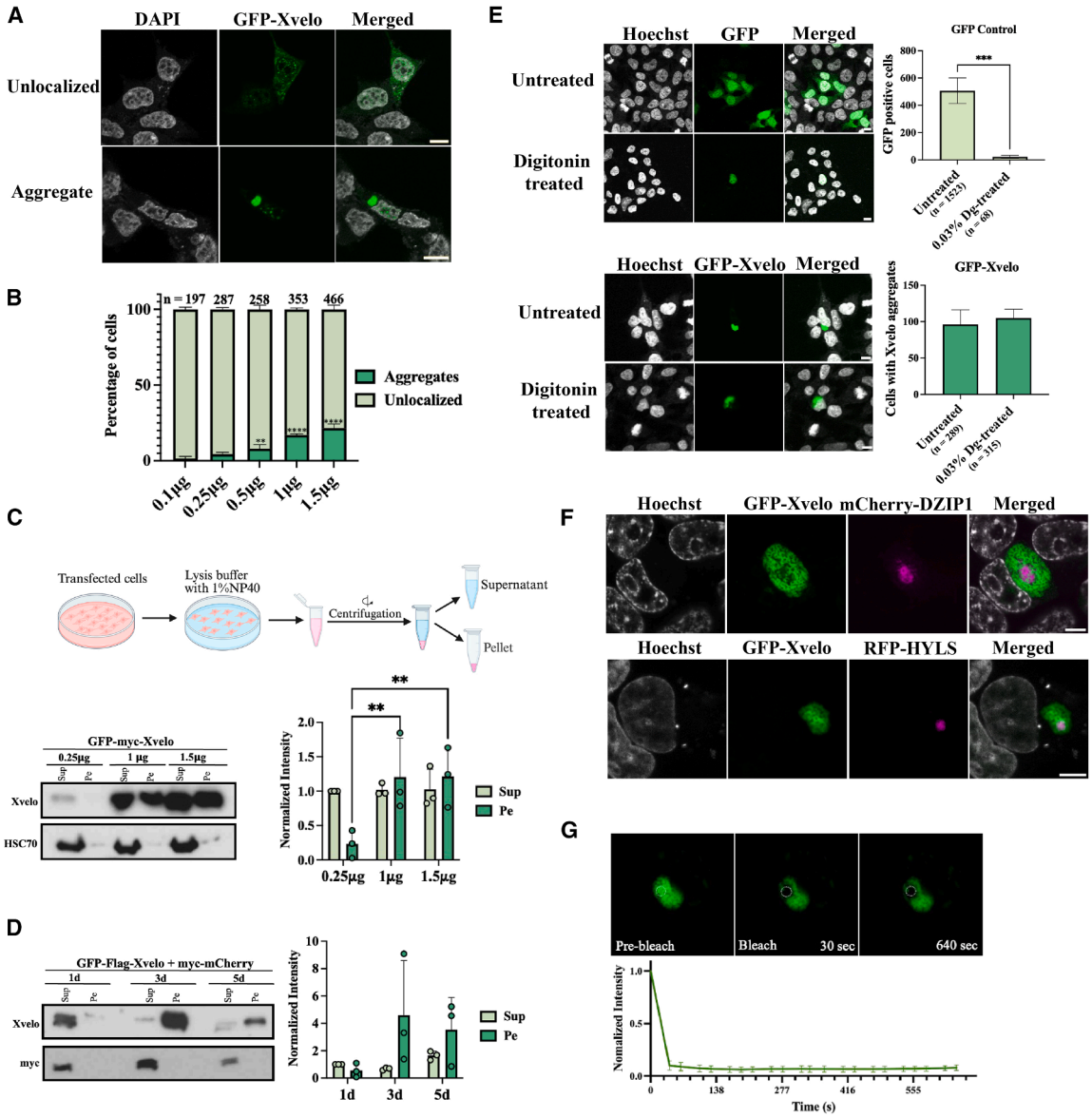


**Figure 1. GFP-Xvelo can form assemblies around the centrosome in cultured HEK293T cells**

(A) Representative images of Xvelo aggregates and unlocalized Xvelo in HEK293T cells are shown.

(B) Bar graph shows the quantification of dose-dependent aggregation of Xvelo as percentages of cells with unlocalized and aggregated Xvelo. The numbers of cells counted are listed on top of each bar graph. Statistical analysis was performed using two-way ANOVA, followed by Fisher's LSD post hoc test using GraphPad Prism (****$p < 0.0001$ and **$p < 0.01$).

(C) Schematic for the fractionation protocol for the separation of soluble and insoluble protein aggregates is shown in the top panel. The effect of increasing Xvelo concentration on the assembly of Xvelo aggregates was assessed by fractionation and western blot on the lower left panel. Quantification of the western blot results is shown in the bar graph on the lower right panel.

(D) Fractionation and western blot results show a gradual accumulation of Xvelo assemblies within the first three days post transfection. By five days post transfection, Xvelo assemblies are partially degraded. Quantifications of immunoblots from three individual experiments are shown on the right. Statistical analysis for 1C and 1D was performed by using two-way ANOVA, followed by Fisher's LSD post hoc test using GraphPad Prism (**p < 0.01).

(E) Representative images for the effect of digitonin (0.3%) extraction of Xvelo assemblies (lower panel) and GFP control (upper panel) are shown. The cells were treated with 0.3% Digitonin containing PBS for 1 min. Bar graphs on the right show quantifications of the result. GFP in the majority of the cells was extracted by the digitonin-treatment. Unpaired *t*-tests were performed on GraphPad Prism for statistical analysis (***$p = 0.0009$).

(F) Co-expression of DZIP1 or HYLS along with GFP-Xvelo was conducted to observe the location of the centrosome with respect to Xvelo assembly.

(G) Normalized intensity of GFP fluorescence in the Xvelo aggregates was followed post photobleaching ($n = 6$).

Representative images are shown in the upper panel. Data are represented as mean ± SD. Scale bars: (1A and 1E): 10 µm; (1F): 5 µm.

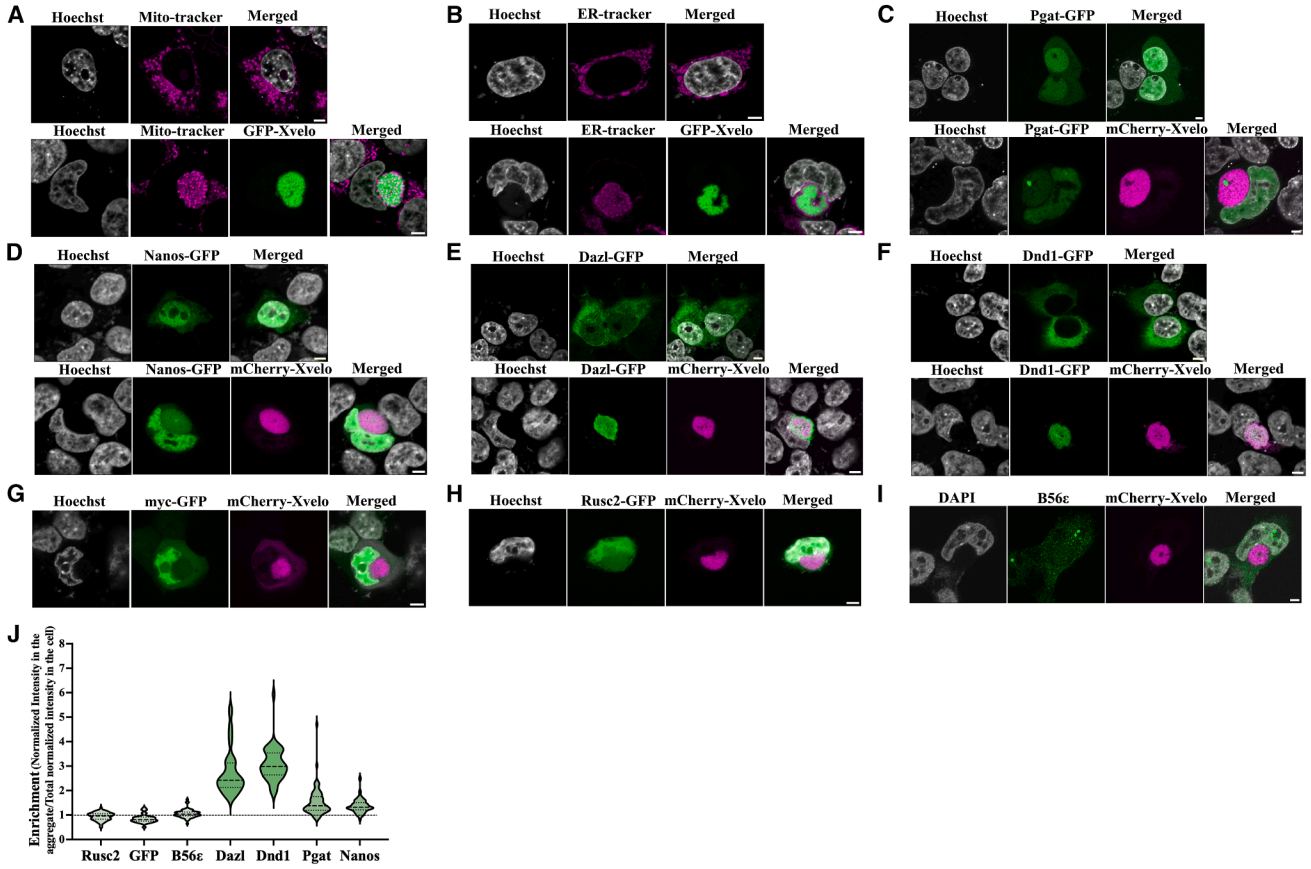


**Figure 2. GFP-Xvelo assembles into "Balbiani body-like" aggregates in HEK293T cells**

A and B are representative images to show the subcellular distribution of mitochondria (A) and ER (B) in control cells (upper panels) and GFP-Xvelo transfected cells (lower panels). Both mitochondria and ER were spread in the entire cytoplasm in control cells, but were recruited into the GFP-Xvelo assembly in GFP-Xvelo transfected cells.

(C–F) are representative images to show the subcellular distribution of germline determinants, including Pgat (C), Nanos (D), Dazl (E), and Dnd1 (F). Upper panels show the distribution of germline determinants when they were expressed alone. Lower panels show their distribution when co-expressed with mCherry-Xvelo.

(G–I) are representative images to show co-expression of mcherry-Xvelo with non-germline proteins, including co-transfected myc-GFP (G), co-transfected Rusc2-GFP (H), and an endogenous protein B56ε (I).

(J) Violin plot shows the enrichment analysis for germline and non-germline protein measured as the normalized intensity of fluorescence of the protein in the aggregate/normalized intensity of fluorescence of the protein in the entire cell. The dotted line represents "No enrichment" i.e., intensity in the aggregate is similar to overall intensity in the cell. Number of aggregates quantified for this analysis (n) = Rusc2 (63), GFP (35), B56ε (67), Dazl (41), Dnd1 (46), Pgat (72), and Nanos (79). Scale bars: 5 μm.

structure in HEK293T cells. In order to further test if this function of Xvelo is specific to the context of HEK293T cells, we performed similar experiments in HeLa cells. We observed that Xvelo assembled around the centrosome (Figure S1A) and enriched mitochondria and ER in HeLa cells as well (Figures S1B and S1C). Thus, the ability of Xvelo assembly to sequester organelles does not require any oocyte-specific factors and is independent of cell context.

One of the most important roles of the Bb is to enrich germline determinants and control their asymmetric localization in the oocyte. To determine if the Xvelo assemblies in somatic cells behave like the Bb in this aspect, we asked if they could selectively recruit germ plasm components. To test this, we transfected cells with Xvelo, along with germ plasm components, including Pgat,[78] xDazl,[79] Nanos1,[80] or Dnd1.[81,82] When expressed alone in HEK293T cells, Pgat and Nanos1 were distributed in both the nucleus and cytoplasm, with a higher level of protein being detected in the nucleus (Figures 2C and 2D). When co-expressed with Xvelo, all cytosolic Pgat and Nanos1 proteins were enriched in the Xvelo aggregates (Figures 2C and 2D). Unlike Pgat and Nanos1, xDazl was highly enriched in the cytoplasm (Figure 2E), and Dnd1 was exclusively present in the cytoplasm (Figure 2F). In cells with Xvelo aggregates, xDazl and Dnd1 were completely enriched in the Xvelo aggregates (Figures 2E and 2F). We counted the percentage of cells in which these germ plasm components colocalized with Xvelo aggregates. We found that 97.4% ($n$ = 192) of Pgat, 98.9% ($n$ = 273) of Nanos1, 99.5% ($n$ = 195) of xDazl, and 98.5% ($n$ = 196) of Dnd1 were enriched in Xvelo aggregates. Additionally, this ability of Xvelo assemblies to enrich germ plasm components is not

specific to HEK293T cells. We also observed an enrichment of xDazl in the Xvelo aggregates in HeLa cells (Figure S1F). To determine if Xvelo assemblies can recruit non-germline proteins, we co-expressed GFP-myc and hRusc-GFP[83] with mCherry-Xvelo. Neither GFP nor hRusc-GFP was enriched in the Xvelo aggregates (Figures 2G and 2H). Furthermore, we examined the localization of the B56ε regulatory subunit of PP2A, an endogenous protein that is ubiquitously expressed in the cell (Figure 2I). B56ε did not show a preference for recruitment into the assemblies either. We performed enrichment analysis to further quantify the enrichment of these proteins in Xvelo aggregates, relative to that in the entire cell (Figure 2J). This analysis clearly suggested a preference for the recruitment of germline determinants into Xvelo aggregates. Of note, although the cytoplasmic Nanos and Pgat were recruited into Xvelo aggregates, the nuclear Nanos and Pgat remained in the nucleus (Figures 2C and 2D). For this reason, the overall enrichment of Nanos and Pgat is less obvious as compared to that of Dazl and Dnd1 (Figure 2J). A similar observation was made when the analysis was performed using HeLa cells (Figures S1D–S1G). Based on the aforementioned findings, we conclude that Xvelo can function as an organizer to assemble a ''Bb-like structure'' in somatic cells and this structure shares key features of the oocyte Bb.

## Centrosome proteins promote assembly of Xvelo

Even after more than a century of the discovery of Bb,[21,84] we do not fully understand the mechanism of its initial assembly. From ultra-structural studies, it was noted that the Bb assembles near the nucleus, around the centrosome.[21,51,85] A recent study showed that dynein-mediated transport of Buc condensates along the microtubules regulates the growth and maturation of Bb in zebrafish oocytes.[50] In our studies in cell culture, we noticed that Xvelo assembles around the centrosome. This led us to speculate that centrosome components could potentially assist in the Bb assembly. Since the Xvelo assemblies in somatic cells resemble the endogenous *Xenopus* and zebrafish Bb, we took advantage of this system to determine if centrosome components could assist in the assembly of Bb. We took a candidate approach and selected a few proteins that localize to different parts of the centrosome. We co-expressed these proteins in cells with Xvelo and tested if any of these components could influence the assembly of Xvelo by quantifying the percentage of cells with aggregated or unlocalized Xvelo (Figure 3A). Xvelo, on its own, formed aggregates in 10% or fewer cells. We found that overexpression of Sas6,[65] cenexin,[86,87] DZIP1,[67] or PLK4[60,88] was able to promote assembly of Xvelo. Sas6 showed the most prominent effect, with nearly 40% of the cells forming aggregates. Another centrosome protein Cep164,[89] however, showed minimal effect on Xvelo assembly (Figure 3A). We further validated these results biochemically by comparing insoluble and soluble Xvelo protein in a fractionation assay (same as Figure 1C). Overexpression of Sas6, DZIP1, and cenexin increased Xvelo in the insoluble (pellet) fraction (Figure 3B). Of note, while quantification of western blot results shows that the effect of DZIP1 on Xvelo aggregation is statistically non-significant, this effect is highly reproducible. Collectively, these results suggest that a subset of centrosome proteins could promote Xvelo assembly.

## Centrosome proteins act on different domains of Xvelo to promote its assembly

Since Sas6, DZIP1, and cenexin promote the assembly of Xvelo, we explored their interaction with Xvelo. Xvelo has a PLD in the N-terminus, which is involved in its self-assembly, and a C-terminal IDR[39] (Figure 4A). We started by testing if the N- (termed as F12) or the C-terminal (F34) half of the protein was sensitive to the over-expression of Sas6, DZIP1, and cenexin. We found that overexpression of Sas6 and cenexin promoted the assembly of both F12 and F34, while DZIP1 could only induce assembly of F34 (Figure 4B). Notably, while the effect of cenexin on F12 is reproducible, it is relatively weak and statistically non-significant. To determine if Sas6 and cenexin act on the PLD to induce Xvelo assembly, we performed a similar experiment with F1, which contains the PLD, and F2, which lacks the PLD (Figure 4A). Indeed, we found Sas6 and cenexin increased the amount of insoluble F1 without affecting the solubility of F2 (Figure 4C). The effect of cenexin is again relatively weak and statistically non-significant. It appears that Sas6 and cenexin can act on the PLD to induce Xvelo assembly. Since Sas6, DZIP1, and cenexin can promote the assembly of the C-terminal of Xvelo protein, we further tested their effects on the assembly of F3 and F4 fragments. We found that overexpression of Sas6, DZIP1, and cenexin increased the amount of insoluble F3 and F4 in a highly reproducible fashion (Figure 4C). Nonetheless, due to the variation among individual experiments, the effect of DZIP1 on F3 and the effects of Sas6 and cenexin on F4 are statistically non-significant. To strengthen our conclusion, we took an imaging approach to analyze the effects of centrosome proteins on Xvelo domains. By quantifying the percentage of cells containing Xvelo aggregates, we found that Sas6 promoted F1 aggregation significantly. Cenexin and DZIP1 induced a significant increase in the percentage of cells with F34 aggregates (Figure 4D).

As Sas6, cenexin, and DZIP1 can act on different domains of Xvelo to induce Xvelo assembly, we went on to determine if these centrosome proteins physically interact with Xvelo. We generated glutathione S-transferase (GST)-tagged Xvelo F1, F3, and F4 and performed GST-pull down experiments. We found that Sas6 interacted with F1, F3, and F4 of Xvelo. DZIP1 interacted with both F3 and F4. Cenexin interacted with F3 strongly, but bound F4 relatively weakly (Figure 4E). Collectively, our results show that different proteins in the centrosome can interact with Xvelo and promote its assembly. We speculate that by binding to Xvelo and enhancing its assembly, centrosome proteins assist in the formation of Bb around the centrosome early in oogenesis.

## Knockdown of centrosome proteins reduces Xvelo assembly

The aforementioned studies demonstrate that Xvelo assembles into a Bb-like structure around the centrosome, and a subset of centrosome proteins, including Sas6, DZIP1, and cenexin, can interact with and promote Xvelo assembly. We further set out to determine if Sas6, DZIP1, and cenexin are required for Xvelo assembly in HEK293T cells. We performed shRNA-mediated knockdown of Sas6, DZIP1, and cenexin (Figure 5B) and asked if depleting these centrosome proteins could deter the

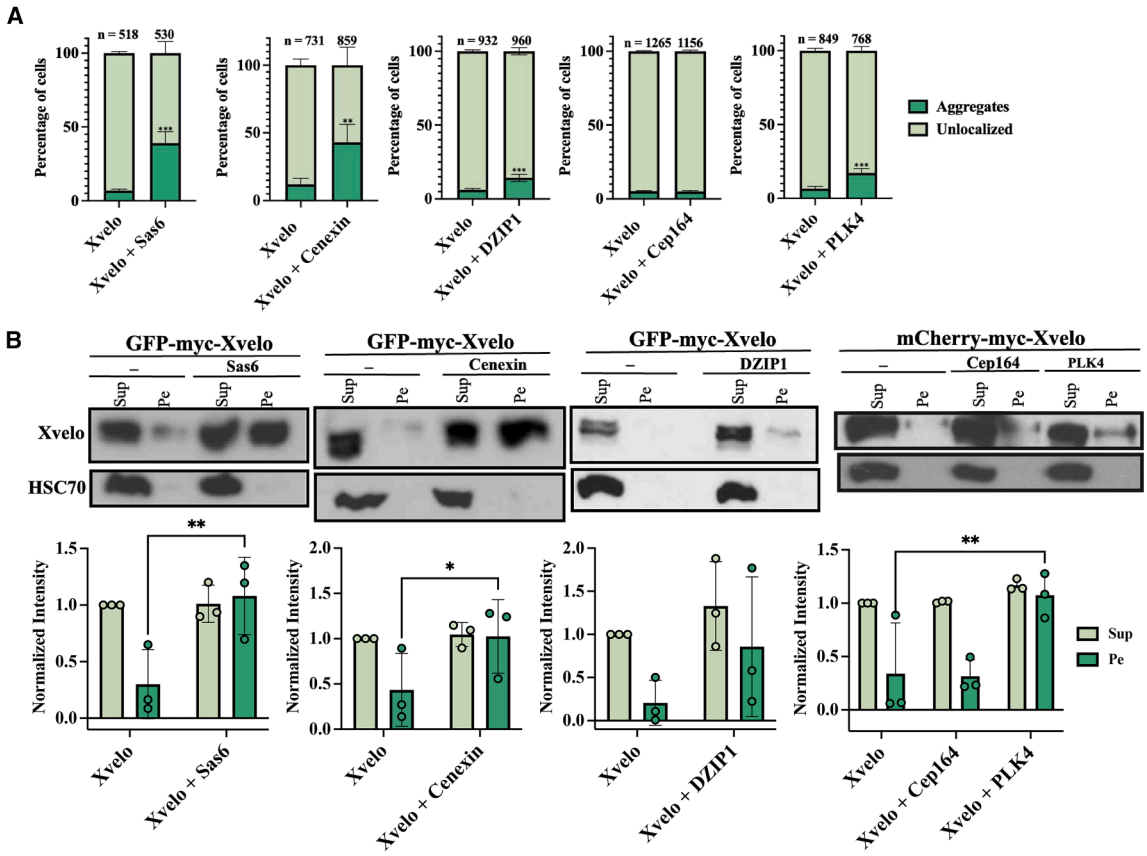


**Figure 3. Co-expression of centrosome components can promote the assembly of Xvelo in HEK293T cells**

(A) Bar graphs show the effects of overexpression of Sas6, PLK4, cenexin, DZIP1, and Cep164 on the aggregation of Xvelo. Xvelo along with a control plasmid or centrosomal components was transfected into HEK293T cells and fixed 24h post transfection. The cells showing unlocalized Xvelo or Xvelo aggregates were counted under the microscope. The total number of cells analyzed from 3 individual experiments is listed on top of each bar graph. Statistical analysis for 1A and 1B was performed using two-way ANOVA, followed by Fisher's LSD post hoc test using GraphPad Prism (***$p < 0.001$ and **$p < 0.01$ and *$p < 0.05$).

(B) The effects of overexpression of Sas6, PLK4, cenexin, xDZIP1, and Cep164 on the assembly of Xvelo were assessed by fractionation and western blot. HSC70, a protein highly enriched in the soluble fraction, was used as a loading control. Quantifications of immunoblots from three experiments are shown under the western blot images. Data are represented as mean ± SD.

assembly of Xvelo. For this experiment, HEK293T cells were transfected with GFP-Flag-Xvelo and then infected with lentiviral shRNAs against *sas6*, *dzip1*, and *cenexin.* Three days post infection, cells were harvested for fractionation and western blot analysis (Figure 5A). We found that while the knockdown of DZIP1 only had a marginal effect, the knockdown of Sas6 and cenexin dramatically reduced the amount of Xvelo in the insoluble fraction (Figure 5C). Knockdown of Sas6, cenexin, and DZIP1 in combination was able to reduce the amount of Xvelo in the pellet even further (Figure 5C). The fact that Sas6, cenexin, and DZIP1 are required for Xvelo assembly provides strong support for our hypothesis that the centrosome assists in Bb formation by promoting Xvelo assembly.

## DISCUSSION

The Bb is a highly conserved physiological amyloid in the oocyte. While the Bb was first discovered in the 1800s,[21] the mechanism governing its initial assembly is not well understood. It is known that the Bb accumulates germline determinants needed for the germ cell specification[30,33,90] and is crucial for the proper localization of these determinants in the oocytes of organisms such as *Xenopus* and zebrafish.[10,22,24] In these species, the initial assembly of the Bb occurs around the centrosome during early oogenesis.[51,52] This event also marks the point of oocyte symmetry break and the establishment of the animal/vegetal axis of the oocyte.[30,33,44] Subsequently, the Bb breaks into numerous small 'germ plasm islands', which are transported to and stored at the vegetal cortex of the oocyte.[90] During the oocyte-to-embryo transition, vegetally localized germ plasm undergoes drastic remodeling. Ultimately, the majority of 'germ plasm islands' are eliminated in the somatic tissues.[91,92] The remaining islands coalesce into large aggregates and are inherited by a few cells in the embryo, leading to the specification of the PGCs. It is known that *Xenopus* Xvelo and its zebrafish homolog Buc function as the matrix protein for the Bb and germ plasm.[33,39,45] In fact, when overexpressed in fertilized eggs where all germ plasm components needed to specify PGCs were available, Buc was

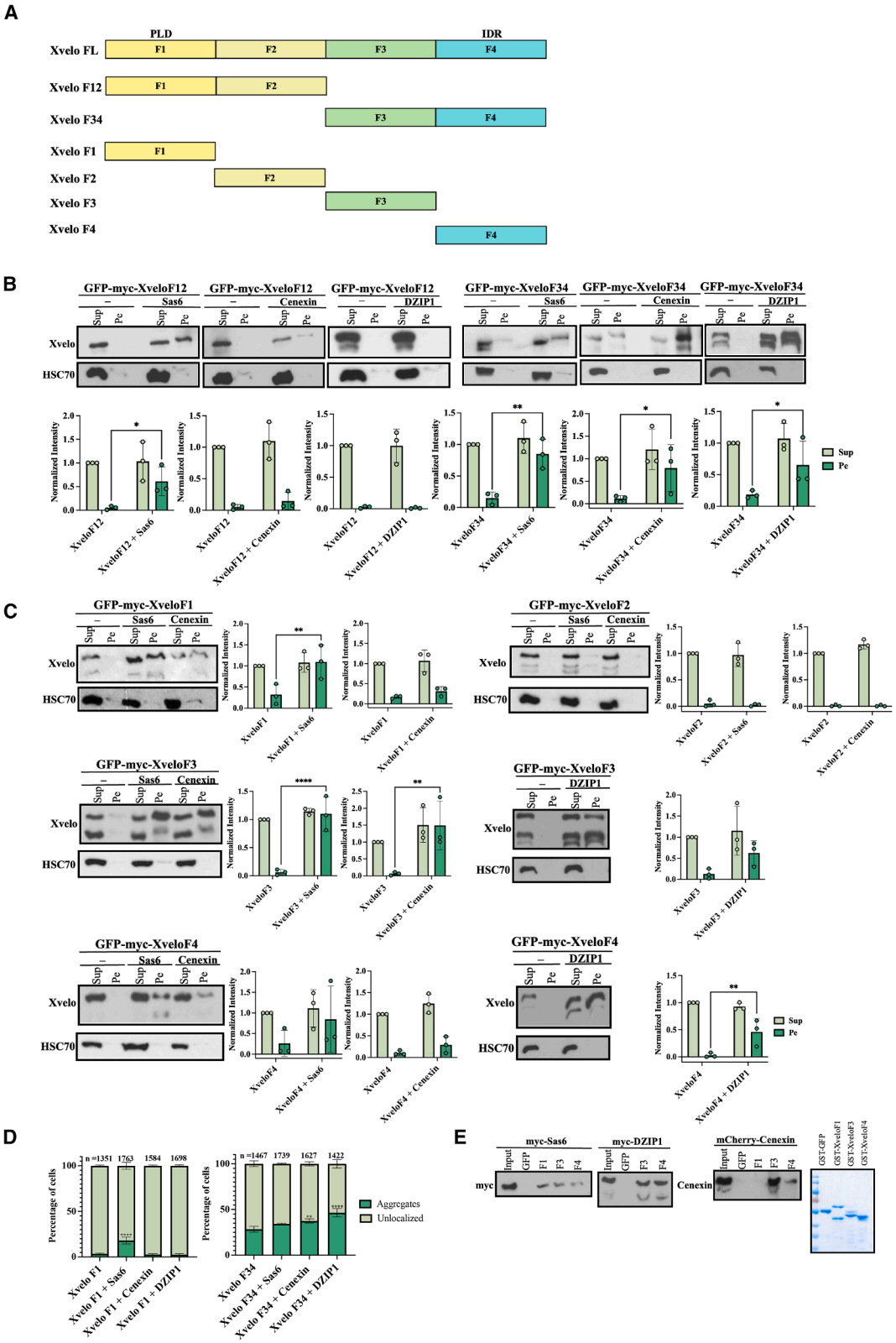


*(legend on next page)*

sufficient for germ plasm assembly, inducing ectopic PGCs in early zebrafish embryos.[33,40,41] Nonetheless, it was unclear if Buc alone is sufficient for the assembly of a Bb in the absence of other germline components.

In this work, we study the assembly of Xvelo in mammalian somatic cells, which lack germ plasm components and other oocyte-specific factors. We found that Xvelo alone was sufficient to reconstitute a "Bb-like" structure in the mammalian somatic cells. These Bb-like assemblies are reminiscent of the Bb in *Xenopus* and zebrafish early oocytes. They form around the centrosome and are capable of recruiting cellular organelles such as mitochondria and ER. Moreover, these Xvelo assemblies can enrich co-expressed germ plasm components such as Dazl, Pgat, Dnd1, and Nanos without affecting the subcellular distribution of non-germline factors. Our FRAP experiment further demonstrates that these Bb-like structures were extremely stable and recovered poorly after photo-bleaching. These findings strongly argue that the assembly of a Bb relies entirely on the biophysical properties of Xvelo/Buc.

The Xvelo protein has an N-terminal PLD that can self-assemble into micron-scale amyloid-like networks *in vitro*.[39] In *Xenopus* oocytes, the PLD is necessary and sufficient for the localization of Xvelo to the Bb. Interestingly, the PLD alone cannot recruit mitochondria and mRNAs. The C-terminal region of Xvelo is essential for these functions.[39] Our work here reveals that both the PLD and the C-terminal portion of Xvelo are required for the assembly of a Bb-like structure in mammalian somatic cells. The PLD can promote self-assembly while interacting with centrosome components such as Sas6 to further increase Xvelo assembly. The IDR-bearing C-terminal region of Xvelo can provide interaction opportunities with additional centrosome components such as DZIP1 and cenexin. We speculate that the interactions between Xvelo and these centrosome proteins are important, as they can recruit Xvelo to the centrosome and initiate Bb formation by enhancing the assembly of Xvelo. In support of this view, we found that overexpression of Sas6, cenexin and DZIP1 enhanced Xvelo assembly, whereas the knockdown of Sas6, cenexin and DZIP1 reduced it. As multiple centrosome components can interact with Xvelo and promote its assembly, the centrosome can act as a Xvelo assembly center to direct the initiation of the Bb formation.

During the final stage of our manuscript preparation, Kar et al.[50] reported a mechanism for the maturation of the Bb in zebrafish. It was demonstrated elegantly that once Bb assembly is initiated, small Buc protein condensates in the oocyte utilize a dynein-mediated transport mechanism to join the existing Bb, leading to the growth and maturation of the Bb. Thus, our findings presented here and the results in the literature collectively support the following model. During the early stages, centrosome proteins such as Sas6, cenexin, and DZIP1 promote assembly of Xvelo/Buc to initiate Bb formation around the centrosome. Subsequently, the centrosome acts as MTOC to facilitate dynein-dependent transport of Buc/Xvelo granules.[50] This eventually gathers all Xvelo/Buc protein condensates around the centrosome, leading to the formation of a mature Bb in the perinuclear region of the oocyte.

Oocytes are post-mitotic cells that can be arrested at prophase I of meiosis I for a long time.[93] Previous studies have demonstrated that the assembly of Bb occurs between the pachytene and diplotene stages of meiosis.[52] While it is not clear why Bb assembly can only happen during this specific window of time, it is possible that Bb assembly is influenced by cell cycle dependent mechanisms. In agreement with this hypothesis, results from our preliminary studies (data not shown) suggest that the assembly of Xvelo aggregates in HEK293T cells is sensitive to cell cycle progression. As centrosome assembly and maturation are dynamically regulated throughout the cell cycle,[94] it would be of great interest to determine if the timing of Bb assembly during oogenesis is determined by a centrosome-dependent regulatory mechanism. Additionally, while Bb has been found in most species, ranging from insects to humans, in the human genome, the Xvelo loci is a pseudo gene. It would be fascinating to investigate if centrosomal proteins regulate Bb assembly in mammals.

## Limitations of the study

It is worth mentioning that our model is based on experiments conducted in mammalian somatic cells. Due to the scope of the current work, we only knocked down cenexin, Sas6, and DZIP1 and investigated their roles in Xvelo assembly in HEK293T cells. In the future, we will carry out loss-of-function experiments in the oocyte and determine if the centrosome facilitates the initiation of Bb formation through the interaction between centrosome proteins and Xvelo/Buc. In addition, since Xvelo interacts with Sas6, cenexin and DZIP1, and possibly some other centrosome proteins, it will be critically important to investigate the dynamic interactions between centrosome and Xvelo/Buc using high-resolution imaging approaches. Even though further work is clearly needed, our study presented

**Figure 4. Centrosome proteins act on different domains of Xvelo to promote its assembly in HEK293T cells**

(A) Schematic representation of the full-length Xvelo (779 amino acid residues) and different fragments is shown. Xvelo F12 (1–410 aa), Xvelo F34 (386–779 aa), Xvelo F1 (1–160 aa), Xvelo F2 (138–410 aa), Xvelo F3 (386–610 aa) and Xvelo F4 (586–779 aa).

(B) The effects of overexpression of Sas6, cenexin, PLK4, DZIP1, and Cep164 on the aggregation of the N-terminus (F12) or C-terminus of Xvelo (F34) were assessed by fractionation and western blot.

(C) The effects of overexpression of Sas6, cenexin, PLK4, DZIP1, and Cep164 on the assembly of the different fragments of Xvelo (F1, F2, F3, and F4) were assessed by fractionation and western blot. Quantifications of immunoblots from three individual experiments are shown under each representative blot.

(D) Bar graphs show the effects of overexpression of Sas6, cenexin and DZIP1 on the aggregation of Xvelo fragments F1 and F34. Cells were transfected with Xvelo constructs along with a control plasmid or centrosomal components, fixed 24h post transfection, and analyzed by imaging. The cells showing unlocalized or aggregated Xvelo were counted under the microscope. The total number of cells analyzed from 3 experiments is listed on top of each bar graph.

(E) GST pull-down and western blot were performed to test for physical interaction between Xvelo fragments and Sas6, cenexin and DZIP1. Coomassie brilliant blue staining to estimate protein concentration is shown in the lower right panel. Statistical analysis in B, C, and D was performed using two-way ANOVA, followed by Fisher's LSD post hoc test using GraphPad Prism (****$p < 0.0001$, ***$p < 0.001$, **$p < 0.01$, and *$p < 0.05$). Data are represented as mean ± SD.

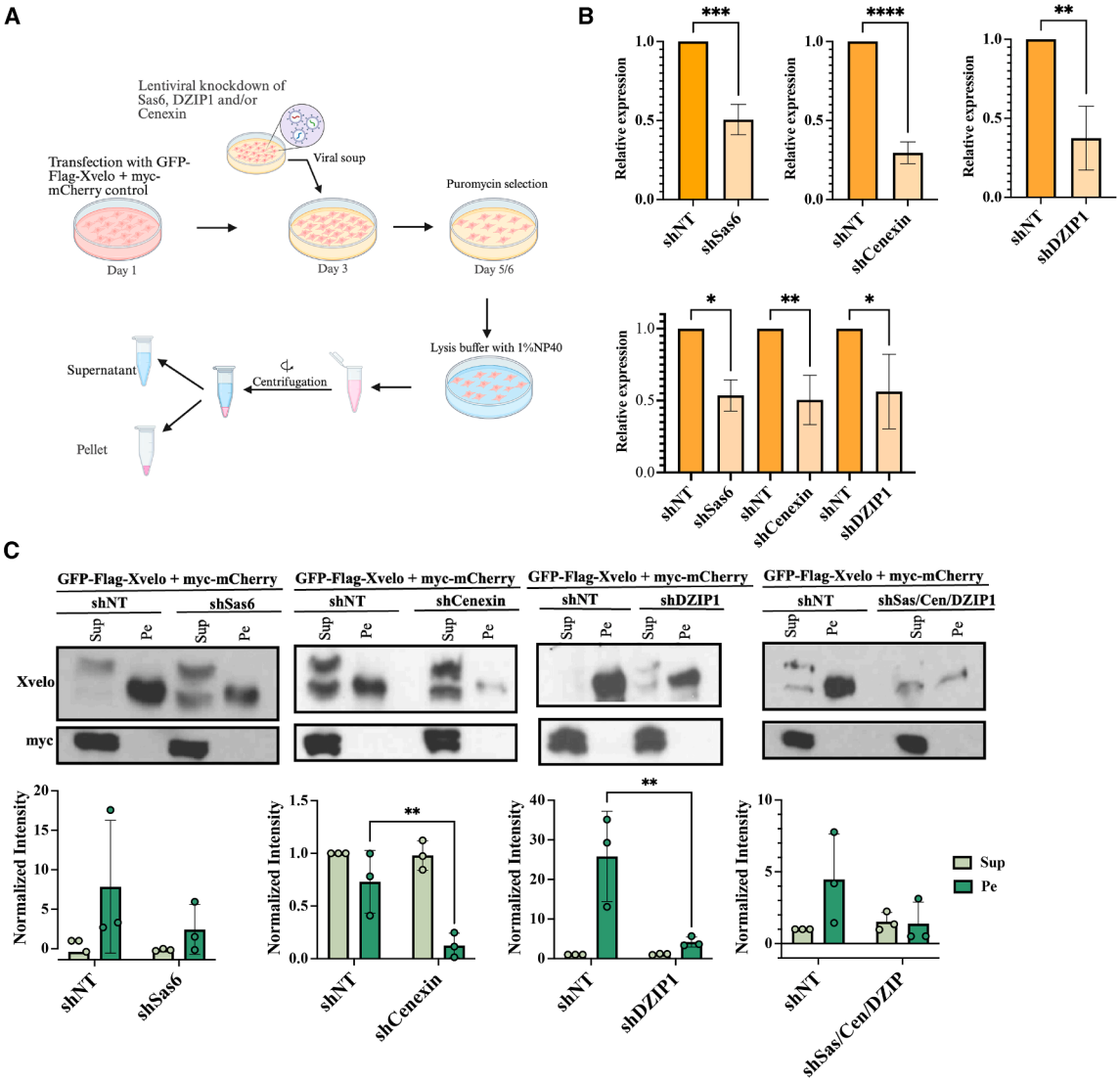


**Figure 5. Knockdown of centrosome components impairs the ability of Xvelo to assemble in HEK293T cells**

(A) Schematic for the experimental procedure of the knockdown experiment.

(B) qPCR validation of knockdown for individual centrosome components (Sas6, cenexin, DZIP1) in the top panel and knockdown of all three in the bottom panel are shown. shNT (Non-Target) represents the control shRNA for this experiment.

(C) Cells with knockdown for Sas6, cenexin, and DZIP1 individually, or in combination were fractionated, followed by western blot analysis. Western blots to assess the assembly of Xvelo are shown. Myc-mCherry was used as a control for transfection and loading. Statistical analysis for 5B and 5C was performed using two-way ANOVA, followed by Fisher's LSD post hoc test using GraphPad Prism (****$p < 0.0001$, ***$p < 0.001$, **$p < 0.01$ and *$p < 0.05$). Although the results shown in the representative immunoblots were highly reproducible, due to variations in knockdown efficiencies among different experiments, statistical analysis concluded no significant difference for Sas6 knockdown and knockdown of all three. Data are represented as mean ± SD.

here provides a model to explain the molecular mechanism governing the initiation of Bb assembly.

## RESOURCE AVAILABILITY

### Lead contact

Further information and requests for resources and reagents should be directed to, and will be fulfilled by the lead contact, Jing Yang (yangj@illinois.edu).

### Materials availability

This study did not generate any unique reagents.

### Data and code availability

- The authors declare that all data supporting the results in this study are available within the paper or its supplemental information.
- This paper does not report any original code.
- Any additional information is available from the lead contact upon request.

## ACKNOWLEDGMENTS

This work is supported by a grant from NIH (R35 GM131810). We appreciate Dr. Brian Mitchell for providing HYLS and Sas6 expression constructs.

## AUTHOR CONTRIBUTIONS

Conceptualization, Divyanshi and J.Y.; data curation, Divyanshi and M.L.; formal analysis, Divyanshi, M.L., and J.Y.; funding acquisition, J.Y.; investigation, Divyanshi and M.L.; methodology, Divyanshi and J.Y.; project administration, Divyanshi and J.Y.; resources, E.B. and J.Y.; supervision, J.Y.; validation, Divyanshi and M.L.; writing – original draft, Divyanshi; writing – review and editing, Divyanshi and J.Y.

## DECLARATION OF INTERESTS

The authors declare no competing interests.

## STAR★METHODS

Detailed methods are provided in the online version of this paper and include the following:

- KEY RESOURCES TABLE
- EXPERIMENTAL MODEL AND STUDY PARTICIPANT DETAILS
  - Cell culture and transfection
- METHOD DETAILS
  - Cellular fractionation
  - Western Blot
  - Mito-tracker and ER tracker staining
  - Fluorescence recovery after photo bleaching (FRAP)
  - Immunostaining
  - Lentiviral knockdown
  - GST pulldown
- QUANTIFICATION AND STATISTICAL ANALYSIS

## SUPPLEMENTAL INFORMATION

Supplemental information can be found online at https://doi.org/10.1016/j.isci.2025.113805.

Received: March 9, 2025
Revised: July 18, 2025
Accepted: October 15, 2025
Published: October 16, 2025

## REFERENCES

1. Gomes, E., and Shorter, J. (2019). The molecular language of membraneless organelles. J. Biol. Chem. *294*, 7115–7127. https://doi.org/10.1074/JBC.TM118.001192.
2. Boeynaems, S., Alberti, S., Fawzi, N.L., Mittag, T., Polymenidou, M., Rousseau, F., Schymkowitz, J., Shorter, J., Wolozin, B., Van Den Bosch, L., et al. (2018). Protein Phase Separation: A New Phase in Cell Biology. Trends Cell Biol. *28*, 420–435. https://doi.org/10.1016/j.tcb.2018.02.004.
3. Li, X.H., Chavali, P.L., Pancsa, R., Chavali, S., and Babu, M.M. (2018). Function and Regulation of Phase-Separated Biological Condensates. Biochemistry *57*, 2452–2461. https://doi.org/10.1021/acs.biochem.7b01228.
4. Hnisz, D., Shrinivas, K., Young, R.A., Chakraborty, A.K., and Sharp, P.A. (2017). A Phase Separation Model for Transcriptional Control. Cell *169*, 13–23. https://doi.org/10.1016/J.CELL.2017.02.007.
5. Sabari, B.R., Dall'Agnese, A., Boija, A., Klein, I.A., Coffey, E.L., Shrinivas, K., Abraham, B.J., Hannett, N.M., Zamudio, A.V., Manteiga, J.C., et al. (2018). Coactivator condensation at super-enhancers links phase separation and gene control. Science *361*, eaar3958. https://doi.org/10.1126/SCIENCE.AAR3958.
6. Youn, J.Y., Dyakov, B.J.A., Zhang, J., Knight, J.D.R., Vernon, R.M., Forman-Kay, J.D., and Gingras, A.C. (2019). Properties of Stress Granule and P-Body Proteomes. Mol. Cell *76*, 286–294. https://doi.org/10.1016/J.MOLCEL.2019.09.014.
7. Ivanov, P., Kedersha, N., and Anderson, P. (2019). Stress Granules and Processing Bodies in Translational Control. Cold Spring Harb. Perspect. Biol. *11*, a032813. https://doi.org/10.1101/CSHPERSPECT.A032813.
8. Ross, C.A., and Poirier, M.A. (2004). Protein aggregation and neurodegenerative disease. Nat. Med. *10*, S10–S17. https://doi.org/10.1038/nm1066.
9. Vaquer-Alicea, J., and Diamond, M.I. (2025). Propagation of Protein Aggregation in. Neurodegener. Dis. *37*, 4. https://doi.org/10.1146/annurev-biochem-061516.
10. Pamula, M.C., and Lehmann, R. (2024). How germ granules promote germ cell fate. Nat. Rev. Genet. *25*, 803–821. https://doi.org/10.1038/s41576-024-00744-8.
11. So, C., Cheng, S., and Schuh, M. (2021). Phase Separation during Germline Development. Trends Cell Biol. *31*, 254–268. https://doi.org/10.1016/J.TCB.2020.12.004.
12. Cassani, M., and Seydoux, G. (2022). Specialized germline P-bodies are required to specify germ cell fate in Caenorhabditis elegans embryos. Development (Camb.) *149*, dev200920. https://doi.org/10.1242/dev.200920.
13. Illmensee, K., and Mahowald, A.P. (1974). Transplantation of posterior polar plasm in Drosophila. Induction of germ cells at the anterior pole of the egg. Proc. Natl. Acad. Sci. USA *71*, 1016–1020. https://doi.org/10.1073/PNAS.71.4.1016.
14. Cabral, S.E., Otis, J.P., and Mowry, K.L. (2022). Multivalent interactions with RNA drive recruitment and dynamics in biomolecular condensates in Xenopus oocytes. iScience *25*, 104811. https://doi.org/10.1016/J.ISCI.2022.104811.
15. Neil, C.R., Jeschonek, S.P., Cabral, S.E., O'Connell, L.C., Powrie, E.A., Otis, J.P., Wood, T.R., and Mowry, K.L. (2021). L-bodies are RNA–protein condensates driving RNA localization in Xenopus oocytes. Mol. Biol. Cell *32*, ar37. https://doi.org/10.1091/MBC.E21-03-0146-T.
16. Painter, T.S. (1924). Studies in mammalian spermatogenesis. V. The chromosomes of the horse. J. Exp. Zool. *39*, 229–247. https://doi.org/10.1002/jez.1400390204.
17. Solari, A.J. (1974). The Behavior of the XY Pair in Mammals. Int. Rev. Cytol. *38*, 273–317.
18. Xu, Y., and Qiao, H. (2021). A Hypothesis: Linking Phase Separation to Meiotic Sex Chromosome Inactivation and Sex-Body Formation. Front. Cell Dev. Biol. *9*, 674203. https://doi.org/10.3389/FCELL.2021.674203.
19. Berchowitz, L.E., Kabachinski, G., Walker, M.R., Carlile, T.M., Gilbert, W.V., Schwartz, T.U., and Amon, A. (2015). Regulated Formation of an Amyloid-like Translational Repressor Governs Gametogenesis. Cell *163*, 406–418. https://doi.org/10.1016/J.CELL.2015.08.060.
20. Carpenter, K., Bell, R.B., Yunus, J., Amon, A., and Berchowitz, L.E. (2018). Phosphorylation-Mediated Clearance of Amyloid-like Assemblies in Meiosis. Dev. Cell *45*, 392–405.e6. https://doi.org/10.1016/j.devcel.2018.04.001.
21. Guraya, S.S. (1979). Recent Advances in the Morphology, Cytochemistry, and Function of Balbiani's Vitelline Body in Animal Oocytes. Int. Rev. Cytol. *59*, 249–321. https://doi.org/10.1016/S0074-7696(08)61664-2.
22. Kloc, M., Bilinski, S., and Etkin, L.D. (2004). The Balbiani Body and Germ Cell Determinants: 150 Years Later. Curr. Top. Dev. Biol. *59*, 1–36. https://doi.org/10.1016/S0070-2153(04)59001-4.
23. Boke, E., and Mitchison, T.J. (2017). The balbiani body and the concept of physiological amyloids. Cell Cycle *16*, 153. https://doi.org/10.1080/15384101.2016.1241605.
24. Jamieson-Lucy, A., and Mullins, M.C. (2019). The vertebrate Balbiani body, germ plasm, and oocyte polarity. Curr. Top. Dev. Biol. *135*, 1–34. https://doi.org/10.1016/BS.CTDB.2019.04.003.
25. Divyanshi, Yang, J., and Yang, J. (2024). Germ plasm dynamics during oogenesis and early embryonic development in Xenopus and zebrafish. Mol. Reprod. Dev. *91*, e23718. https://doi.org/10.1002/MRD.23718.
26. Kloc, M., Jedrzejowska, I., Tworzydlo, W., and Bilinski, S.M. (2014). Balbiani body, nuage and sponge bodies – The germ plasm pathway players.

Arthropod Struct. Dev. *43*, 341–348. https://doi.org/10.1016/J.ASD.2013.12.003.

27. De Smedt, V., Szö llö si, D., and Kloc, M. (2000). The Balbiani Body: Asymmetry in the Mammalian Oocyte. Genesis *26*, 208–212. https://doi.org/10.1002/(sici)1526-968x(200003)26:3<208::aid-gene6>3.3.co;2-e.

28. Cox, R.T., and Spradling, A.C. (2003). A Balbiani body and the fusome mediate mitochondrial inheritance duringDrosophila oogenesis. Development *130*, 1579–1590. https://doi.org/10.1242/DEV.00365.

29. Heasman, J., Quarmby, J., and Wylie, C.C. (1984). The mitochondrial cloud of Xenopus oocytes: The source of germinal granule material. Dev. Biol. *105*, 458–469. https://doi.org/10.1016/0012-1606(84)90303-8.

30. Marlow, F.L., and Mullins, M.C. (2008). Bucky ball functions in Balbiani body assembly and animal–vegetal polarity in the oocyte and follicle cell layer in zebrafish. Dev. Biol. *321*, 40–50. https://doi.org/10.1016/J.YDBIO.2008.05.557.

31. Pepling, M.E., Wilhelm, J.E., O'Hara, A.L., Gephardt, G.W., and Spradling, A.C. (2007). Mouse oocytes within germ cell cysts and primordial follicles contain a Balbiani body. Proc. Natl. Acad. Sci. USA *104*, 187–192. https://doi.org/10.1073/PNAS.0609923104.

32. Hertig, A.T. (1968). The primary human oocyte: Some observations on the fine structure of Balbiani's vitelline body and the origin of the annulate lamellae. Am. J. Anat. *122*, 107–137. https://doi.org/10.1002/AJA.1001220107.

33. Bontems, F., Stein, A., Marlow, F., Lyautey, J., Gupta, T., Mullins, M.C., and Dosch, R. (2009). Bucky Ball Organizes Germ Plasm Assembly in Zebrafish. Curr. Biol. *19*, 414–422. https://doi.org/10.1016/j.cub.2009.01.038.

34. Dhandapani, L., Salzer, M.C., Duran, J.M., Zaffagnini, G., de Guirior, C., Martínez-Zamora, M.A., and Böke, E. (2022). Comparative analysis of vertebrates reveals that mouse primordial oocytes do not contain a Balbiani body. J. Cell Sci. *135*, jcs259394. https://doi.org/10.1242/JCS.259394.

35. Lei, L., Ikami, K., Diaz Miranda, E.A., Ko, S., Wilson, F., Abbott, H., Pandoy, R., and Jin, S. (2024). The mouse Balbiani body regulates primary oocyte quiescence via RNA storage. Commun. Biol. *7*, 1247. https://doi.org/10.1038/s42003-024-06900-4.

36. Hill, J.H., Chen, Z., and Xu, H. (2014). Selective propagation of functional mitochondrial DNA during oogenesis restricts the transmission of a deleterious mitochondrial variant. Nat. Genet. *46*, 389–392. https://doi.org/10.1038/ng.2920.

37. Bilinski, S.M., Kloc, M., and Tworzydlo, W. (2017). Selection of mitochondria in female germline cells: is Balbiani body implicated in this process? J. Assist. Reprod. Genet. *34*, 1405–1412. https://doi.org/10.1007/S10815-017-1006-3.

38. Tworzydlo, W., Sekula, M., and Bilinski, S.M. (2020). Transmission of Functional, Wild-Type Mitochondria and the Fittest mtDNA to the Next Generation: Bottleneck Phenomenon, Balbiani Body, and Mitophagy. Genes *11*, 104. https://doi.org/10.3390/GENES11010104.

39. Boke, E., Ruer, M., Wühr, M., Coughlin, M., Lemaitre, R., Gygi, S.P., Alberti, S., Drechsel, D., Hyman, A.A., and Mitchison, T.J. (2016). Amyloid-like Self-Assembly of a Cellular Compartment. Cell *166*, 637–650. https://doi.org/10.1016/J.CELL.2016.06.051.

40. Wang, X., Zhu, J., Wang, H., Deng, W., Jiao, S., Wang, Y., He, M., Zhang, F., Liu, T., Hao, Y., et al. (2023). Induced formation of primordial germ cells from zebrafish blastomeres by germplasm factors. Nat. Commun. *14*, 7918. https://doi.org/10.1038/s41467-023-43587-3.

41. Song, P., Sun, B., Zhu, Y., Zhong, Y., Guo, J., Gui, L., and Li, M. (2021). Bucky ball induces primordial germ cell increase in medaka. Gene *768*, 145317. https://doi.org/10.1016/J.GENE.2020.145317.

42. Nijjar, S., and Woodland, H.R. (2013). Protein interactions in Xenopus germ plasm RNP particles. PLoS One *8*, e80077. https://doi.org/10.1371/journal.pone.0080077.

43. Claußen, M., and Pieler, T. (2010). Identification of vegetal RNA-localization elements in Xenopus oocytes. Methods *51*, 146–151. https://doi.org/10.1016/J.YMETH.2010.02.016.

44. Dosch, R., Wagner, D.S., Mintzer, K.A., Runke, G., Wiemelt, A.P., and Mullins, M.C. (2004). Maternal control of vertebrate development before the midblastula transition: mutants from the zebrafish I. Dev. Cell *6*, 771–780. https://doi.org/10.1016/J.DEVCEL.2004.05.002.

45. Krishnakumar, P., Riemer, S., Perera, R., Lingner, T., Goloborodko, A., Khalifa, H., Bontems, F., Kaufholz, F., El-Brolosy, M.A., and Dosch, R. (2018). Functional equivalence of germ plasm organizers. PLoS Genet. *14*, e1007696. https://doi.org/10.1371/JOURNAL.PGEN.1007696.

46. Han, T.W., Kato, M., Xie, S., Wu, L.C., Mirzaei, H., Pei, J., Chen, M., Xie, Y., Allen, J., Xiao, G., and McKnight, S.L. (2012). Cell-free Formation of RNA Granules: Bound RNAs Identify Features and Components of Cellular Assemblies. Cell *149*, 768–779. https://doi.org/10.1016/J.CELL.2012.04.016.

47. Nott, T.J., Petsalaki, E., Farber, P., Jervis, D., Fussner, E., Plochowietz, A., Craggs, T.D., Bazett-Jones, D.P., Pawson, T., Forman-Kay, J.D., and Baldwin, A.J. (2015). Phase Transition of a Disordered Nuage Protein Generates Environmentally Responsive Membraneless Organelles. Mol. Cell *57*, 936–947. https://doi.org/10.1016/J.MOLCEL.2015.01.013.

48. King, O.D., Gitler, A.D., and Shorter, J. (2012). The tip of the iceberg: RNA-binding proteins with prion-like domains in neurodegenerative disease. Brain Res. *1462*, 61–80. https://doi.org/10.1016/J.BRAINRES.2012.01.016.

49. Li, P., Banjade, S., Cheng, H.-C., Kim, S., Chen, B., Guo, L., Llaguno, M., Hollingsworth, J.V., King, D.S., Banani, S.F., et al. (2012). Phase transitions in the assembly of multivalent signalling proteins. Nature *483*, 336–340. https://doi.org/10.1038/nature10879.

50. Kar, S., Deis, R., Ahmad, A., Bogoch, Y., Dominitz, A., Shvaizer, G., Sasson, E., Mytlis, A., Ben-Zvi, A., and Elkouby, Y.M. (2025). The Balbiani body is formed by microtubule-controlled molecular condensation of Buc in early oogenesis. Curr. Biol. *35*, 315–332.e7. https://doi.org/10.1016/J.CUB.2024.11.056.

51. Kloc, M., Bilinski, S., Dougherty, M.T., Brey, E.M., and Etkin, L.D. (2004). Formation, architecture and polarity of female germline cyst in Xenopus. Dev. Biol. *266*, 43–61. https://doi.org/10.1016/J.YDBIO.2003.10.002.

52. Elkouby, Y.M., Jamieson-Lucy, A., and Mullins, M.C. (2016). Oocyte Polarization Is Coupled to the Chromosomal Bouquet, a Conserved Polarized Nuclear Configuration in Meiosis. PLoS Biol. *14*, e1002335. https://doi.org/10.1371/JOURNAL.PBIO.1002335.

53. Bornens, M. (2012). The Centrosome in Cells and Organisms. Science *335*, 422.

54. Woodruff, J.B., Ferreira Gomes, B., Widlund, P.O., Mahamid, J., Honigmann, A., and Hyman, A.A. (2017). The Centrosome Is a Selective Condensate that Nucleates Microtubules by Concentrating Tubulin. Cell *169*, 1066–1077.e10. https://doi.org/10.1016/J.CELL.2017.05.028.

55. Szollosi, D., Calarco, P., and Donahue, R.P. (1972). Absence of centrioles in the first and second meiotic spindles of mouse oocytes. J. Cell Sci. *11*, 521–541. https://doi.org/10.1242/JCS.11.2.521.

56. Hertig, A.T., and Adams, E.C. (1967). STUDIES ON THE HUMAN OOCYTE AND ITS FOLLICLE I. Ultrastructural and Histochemical Observations on the Primordial Follicle Stage. J. Cell Biol. *34*, 647–675. https://doi.org/10.1083/JCB.34.2.647.

57. Gerhart, J.C., and Goldberger, R.F. (1980). Biological regulation and development. In Mechanisms Regulation Pattern Formation in the Amphibian Egg and Early Embryo (Plenum Press), pp. 133–316.

58. Pimenta-Marques, A., Bento, I., Lopes, C.A.M., Duarte, P., Jana, S.C., and Bettencourt-Dias, M. (2016). A mechanism for the elimination of the female gamete centrosome in Drosophila melanogaster. Science *353*, aaf4866. https://doi.org/10.1126/SCIENCE.AAF4866.

59. Montenegro Gouveia, S., Zitouni, S., Kong, D., Duarte, P., Ferreira Gomes, B., Sousa, A.L., Tranfield, E.M., Hyman, A., Loncarek, J., and

Bettencourt-Dias, M. (2019). PLK4 is a microtubule-associated protein that self-assembles promoting *de novo* MTOC formation. J. Cell Sci. *132*, jcs219501. https://doi.org/10.1242/JCS.219501.

60. Park, J.E., Zhang, L., Bang, J.K., Andresson, T., DiMaio, F., and Lee, K.S. (2019). Phase separation of Polo-like kinase 4 by autoactivation and clustering drives centriole biogenesis. Nat. Commun., 4959. https://doi.org/10.1038/s41467-019-12619-2.
61. Mu, Z., Zheng, P., Liu, S., Kang, Y., and Xie, H. (2025). Plk4 regulates centriole duplication in the embryonic development of zebrafish. Dev. Biol. *517*, 148–156. https://doi.org/10.1016/J.YDBIO.2024.09.006.
62. Aljiboury, A., Mujcic, A., Curtis, E., Cammerino, T., Magny, D., Lan, Y., Bates, M., Freshour, J., Ahmed-Braimeh, Y.H., and Hehnly, H. (2022). Pericentriolar matrix (PCM) integrity relies on cenexin and polo-like kinase (PLK)1. Mol. Biol. Cell *33*, br14. https://doi.org/10.1091/MBC.E22-01-0015.
63. Grzonka, M., and Bazzi, H. (2024). Mouse SAS-6 is required for centriole formation in embryos and integrity in embryonic stem cells. eLife *13*, e94694. https://doi.org/10.7554/ELIFE.94694.
64. Van Breugel, M., Hirono, M., Andreeva, A., Yanagisawa, H.A., Yamaguchi, S., Nakazawa, Y., Morgner, N., Petrovich, M., Ebong, I.O., Robinson, C.V., et al. (2011). Structures of SAS-6 suggest its organization in centrioles. Science *331*, 1196–1199. https://doi.org/10.1126/SCIENCE.1199325.
65. Kitagawa, D., Vakonakis, I., Olieric, N., Hilbert, M., Keller, D., Olieric, V., Bortfeld, M., Erat, M.C., Flückiger, I., Gönczy, P., and Steinmetz, M.O. (2011). Structural basis of the 9-fold symmetry of centrioles. Cell *144*, 364–375. https://doi.org/10.1016/j.cell.2011.01.008.
66. Yabe, T., Ge, X., and Pelegri, F. (2007). The zebrafish maternal-effect gene cellular atoll encodes the centriolar component sas-6 and defects in its paternal function promote whole genome duplication. Dev. Biol. *312*, 44–60. https://doi.org/10.1016/J.YDBIO.2007.08.054.
67. Kim, H.R., Richardson, J., van Eeden, F., and Ingham, P.W. (2010). Gli2a protein localization reveals a role for Iguana/DZIP1 in primary ciliogenesis and a dependence of Hedgehog signal transduction on primary cilia in the zebrafish. BMC Biol. *8*, 65. https://doi.org/10.1186/1741-7007-8-65.
68. Tay, S.Y., Yu, X., Wong, K.N., Panse, P., Ng, C.P., and Roy, S. (2010). The iguana/DZIP1 protein is a novel component of the ciliogenic pathway essential for axonemal biogenesis. Dev. Dyn. *239*, 527–534. https://doi.org/10.1002/dvdy.22199.
69. Glazer, A.M., Wilkinson, A.W., Backer, C.B., Lapan, S.W., Gutzman, J.H., Cheeseman, I.M., and Reddien, P.W. (2010). The Zn Finger protein Iguana impacts Hedgehog signaling by promoting ciliogenesis. Dev. Biol. *337*, 148–156. https://doi.org/10.1016/j.ydbio.2009.10.025.
70. Sekimizu, K., Nishioka, N., Sasaki, H., Takeda, H., Karlstrom, R.O., and Kawakami, A. (2004). The zebrafish iguana locus encodes Dzip1, a novel zinc-finger protein required for proper regulation of Hedgehog signaling. Development *131*, 2521–2532. https://doi.org/10.1242/dev.01059.
71. Schwend, T., Jin, Z., Jiang, K., Mitchell, B.J., Jia, J., and Yang, J. (2013). Stabilization of Speckle-type POZ Protein (Spop) by Daz Interacting Protein 1 (Dzip1) Is Essential for Gli Turnover and the Proper Output of Hedgehog Signaling. J. Biol. Chem. *288*, 32809–32820. https://doi.org/10.1074/JBC.M113.512962.
72. Wolff, C., Roy, S., Lewis, K.E., Schauerte, H., Joerg-Rauch, G., Kirn, A., Weiler, C., Geisler, R., Haffter, P., and Ingham, P.W. (2004). iguana encodes a novel zinc-finger protein with coiled-coil domains essential for Hedgehog signal transduction in the zebrafish embryo. Genes Dev. *18*, 1565–1576. https://doi.org/10.1101/GAD.296004.
73. Jin, Z., Mei, W., Strack, S., Jia, J., and Yang, J. (2011). The antagonistic action of B56-containing protein phosphatase 2As and casein kinase 2 controls the phosphorylation and Gli turnover function of Daz interacting protein. J. Biol. Chem. *286*, 36171–36179. https://doi.org/10.1074/jbc.M111.274761.
74. Wang, C., Low, W.C., Liu, A., and Wang, B. (2013). Centrosomal Protein DZIP1 Regulates Hedgehog Signaling by Promoting Cytoplasmic Retention of Transcription Factor GLI3 and Affecting Ciliogenesis. J. Biol. Chem. *288*, 29518–29529. https://doi.org/10.1074/JBC.M113.492066.
75. Turgeon, A., Fu, J., Yang, J., Ma, M., Ma, M., Jin, Z., Hwang, H., Li, M., Qiao, H., and Mei, W. (2024). Dzip1 is dynamically expressed in the vertebrate germline and regulates the development of Xenopus primordial germ cells. Dev. Biol. *514*, 28–36. https://doi.org/10.1016/J.YDBIO.2024.06.003.
76. Dammermann, A., Pemble, H., Mitchell, B.J., McLeod, I., Yates, J.R., Kintner, C., Desai, A.B., and Oegema, K. (2009). The hydrolethalus syndrome protein HYLS-1 links core centriole structure to cilia formation. Genes Dev. *23*, 2046–2059. https://doi.org/10.1101/GAD.1810409.
77. Heasman, J., Quarmby, J., and Wylie, C.C. (1984). The Mitochondrial Cloud of Xenopus Oocytes: The Source of Germinal Granule Material. Dev. Biol. *105*, 458–469.
78. Hudson, C., and Woodland, H.R. (1998). Xpat, a gene expressed specifically in germ plasm and primordial germ cells of Xenopus laevis. Mech. Dev. *73*, 159–168. https://doi.org/10.1016/S0925-4773(98)00047-1.
79. Houston, D.W., Zhang, J., Maines, J.Z., Wasserman, S.A., and King, M.L. (1998). A Xenopus DAZ-like gene encodes an RNA component of germ plasm and is a functional homologue of Drosophila boule. Development *125*, 171–180. https://doi.org/10.1242/DEV.125.2.171.
80. Mosquera, L., Forristall, C., Zhou, Y., and King, M.L. (1993). A mRNA localized to the vegetal cortex of Xenopus oocytes encodes a protein with a nanos-like zinc finger domain. Development *117*, 377–386. https://doi.org/10.1242/DEV.117.1.377.
81. Horvay, K., Claußen, M., Katzer, M., Landgrebe, J., and Pieler, T. (2006). Xenopus Dead end mRNA is a localized maternal determinant that serves a conserved function in germ cell development. Dev. Biol. *291*, 1–11. https://doi.org/10.1016/J.YDBIO.2005.06.013.
82. Weidinger, G., Stebler, J., Slanchev, K., Dumstrei, K., Wise, C., Lovell-Badge, R., Thisse, C., Thisse, B., and Raz, E. (2003). dead end, a Novel Vertebrate Germ Plasm Component, Is Required for Zebrafish Primordial Germ Cell Migration and Survival Results and Discussion Zebrafish dead end RNA Is a Component of the Germ Plasm and Is Specifically Expressed in Primordial Germ Cells. Curr. Biol. *13*, 1429–1434. https://doi.org/10.1016/S.
83. Jin, Z., Schwend, T., Fu, J., Bao, Z., Liang, J., Zhao, H., Mei, W., and Yang, J. (2016). Members of the rusc protein family interact with Sufu and inhibit vertebrate hedgehog signaling. Development (Camb.) *143*, 3944–3955. https://doi.org/10.1242/dev.138917.
84. Eddy, E.M. (1975). Germ Plasm and the Differentiation of the Germ Cell Line. Int. Rev. Cytol. *43*, 229–280. https://doi.org/10.1016/S0074-7696(08)60070-4.
85. Eddy, E.M. (1974). Fine structural observations on the form and distribution of nuage in germ cells of the rat. Anat. Rec. *178*, 731–757. https://doi.org/10.1002/AR.1091780406.
86. Hüber, D., Geisler, S., Monecke, S., and Hoyer-Fender, S. (2008). Molecular dissection of ODF2/Cenexin revealed a short stretch of amino acids necessary for targeting to the centrosome and the primary cilium. Eur. J. Cell Biol. *87*, 137–146. https://doi.org/10.1016/J.EJCB.2007.10.004.
87. Nakagawa, Y., Yamane, Y., Okanoue, T., Tsukita, S., and Tsukita, S. (2001). Outer dense fiber 2 is a widespread centrosome scaffold component preferentially associated with mother centrioles: Its identification from isolated centrosomes. Mol. Biol. Cell *12*, 1687–1697. https://doi.org/10.1091/MBC.12.6.1687.
88. Sillibourne, J.E., Tack, F., Vloemans, N., Boeckx, A., Thambirajah, S., Bonnet, P., Ramaekers, F.C.S., Bornens, M., and Grand-Perret, T. (2010). Autophosphorylation of polo-like kinase 4 and its role in centriole duplication. Mol. Biol. Cell *21*, 547–561. https://doi.org/10.1091/MBC.E09-06-0505.
89. Graser, S., Stierhof, Y.D., Lavoie, S.B., Gassner, O.S., Lamla, S., Le Clech, M., and Nigg, E.A. (2007). Cep164, a novel centriole appendage protein required for primary cilium formation. J. Cell Biol. *179*, 321–330. https://doi.org/10.1083/JCB.200707181.

90. Wilk, K., Bilinski, S., Dougherty, M.T., and Kloc, M. (2005). Delivery of germinal granules and localized RNAs via the messenger transport organizer pathway to the vegetal cortex of Xenopus oocytes occurs through directional expansion of the mitochondrial cloud. Int. J. Dev. Biol. *49*, 17–21. https://doi.org/10.1387/IJDB.041906KW.

91. Riemer, S., Bontems, F., Krishnakumar, P., Gömann, J., and Dosch, R. (2015). A functional Bucky ball-GFP transgene visualizes germ plasm in living zebrafish. Gene Expr. Patterns *18*, 44–52. https://doi.org/10.1016/j.gep.2015.05.003.

92. Hwang, H., Chen, S., Ma, M., Divyanshi, Fan, H.-C., Borwick, E., Böke, E., Mei, W., and Yang, J. (2023). Solubility phase transition of maternal RNAs during vertebrate oocyte-to-embryo transition. Dev. Cell *58*, 2776–2788. e5. https://doi.org/10.1016/J.DEVCEL.2023.10.005.

93. Wallace, R.A., and Selman, K. (1981). Cellular and Dynamic Aspects of Oocyte Growth in Teleosts. Am. Zool. *21*, 325–343. https://doi.org/10.1093/ICB/21.2.325.

94. Barr, A.R., and Gergely, F. (2007). Aurora-A: the maker and breaker of spindle poles. J. Cell Sci. *120*, 2987–2996. https://doi.org/10.1242/JCS.013136.

95. Jin, Z., Shi, J., Saraf, A., Mei, W., Zhu, G.Z., Strack, S., and Yang, J. (2009). The 48-kDa alternative translation isoform of PP2A:B56ε is required for Wnt signaling during midbrain-hindbrain boundary formation. J. Biol. Chem. *284*, 7190–7200. https://doi.org/10.1074/jbc.M807907200.

96. Aguero, T., Jin, Z., Chorghade, S., Kalsotra, A., King, M.L., and Yang, J. (2017). Maternal dead-end 1 promotes translation of nanos1 by binding the eiF3 complex. Development (Camb.) *144*, 3755–3765. https://doi.org/10.1242/DEV.152611/264481.

97. Schneider, C.A., Rasband, W.S., and Eliceiri, K.W. (2012). NIH Image to ImageJ: 25 years of image analysis. Nat. Methods, 671–671675. https://doi.org/10.1038/nmeth.2089.

## STAR★METHODS

### KEY RESOURCES TABLE

| REAGENT or RESOURCE | SOURCE | IDENTIFIER |
|---|---|---|
| Antibodies | | |
| Rabbit anti-Xvelo | Boke et al.[39] | N/A |
| Mouse anti-HSC70 | Santa Cruz | Cat. Sc-7298; RRID: AB_627761 |
| Rabbit anti-mDZIP1 | Jin et al.[73] | N/A |
| Goat anti-GFP | Rockland | Cat. 600-101-215; RRID: AB_218182 |
| Mouse anti-c-Myc | Thermo Fisher | Cat. 13-2500; RRID:AB_2533008 |
| Rabbit anti-ODF2 (Cenexin) | Thermo Fisher | Cat. 12058-1-AP; RRID:AB_2156630 |
| Rabbit anti-B56ε | Jin et al.[95] | N/A |
| Goat anti-rabbit-488 | Thermo Fisher | Cat. A11008 |
| Secondary anti-rabbit-HRP | GE Healthcare | Cat. NA934V |
| Secondary anti-mouse-HRP | GE Healthcare | Cat. NA931V |
| Chemicals, peptides, and recombinant proteins | | |
| Dulbecco's Modified Eagle Media (DMEM) | Fisher Scientific | Cat. SH30243.01 |
| Foetal Bovine Serum | Fisher Scientific | Cat. FB12999102 |
| Penicillin-Streptomycin | Corning | Cat. 30-001-CI |
| Opti-MEM™ | Thermo Fisher Scientific | Cat. 11058021 |
| Fluorobrite™ DMEM | Thermo Fisher Scientific | Cat. A1896701 |
| Puromycin | Thermo Fisher Scientific | Cat. A1113803 |
| Protease inhibitor cocktail | Sigma | Cat. P8340 |
| Glass bottom dish | MatTek | Cat. P35GC-1.5-14-C |
| Mito-tracker | Thermo Fisher Scientific | Cat. M7512 |
| ER-tracker | Thermo Fisher Scientific | Cat. E34250 |
| Hoechst 33342 | Invitrogen | Cat. H1399 |
| TRIzol reagent | Thermo Fisher Scientific | Cat. 15596018 |
| 2 × SYBR Green qPCR Master Mix | Bimake | Cat. B21203 |
| M-MLV Reverse Transcriptase | Promega | Cat. M1701 |
| ECL™ Prime Western Blotting Detection Reagent | Amersham | Cat. RPN2236 |
| Glutathione Sepharose™ 4B | Sigma | Cat. GE17-0756-01 |
| HEPES | Thermo Fisher Scientific | Cat. BP310 |
| Triton X-100 | Fisher bioreagents | Cat. BP151 |
| Sodium dodecyl sulfate (SDS) | Sigma | Cat. L4390 |
| Polyethylenimine (PEI) | Polysciences | Cat. 23966 |
| Experimental models: Cell lines | | |
| Human: HEK293T cells | ATCC | CRL-3216™ |
| Human: HeLa cells | ATCC | CCL-2™ |
| Oligonucleotides | | |
| See S-Table S1 for a list of oligonucleotides | | |
| Recombinant DNA | | |
| pCS2-GFP-myc-Xvelo | This paper | N/A |
| pCS2-mCherry-myc-Xvelo | Hwang et al.[92] | N/A |
| pCS2-GFP-Flag-Xvelo | This paper | N/A |
| pCS2-GFP-myc-XveloF12 | This paper | N/A |
| pCS2-GFP-myc-XveloF34 | This paper | N/A |
| pCS2-GFP-myc-XveloF1 | This paper | N/A |
| pCS2-GFP-myc-XveloF2 | This paper | N/A |

(*Continued on next page*)

*Continued*

| REAGENT or RESOURCE | SOURCE | IDENTIFIER |
|---|---|---|
| pCS2-GFP-myc-XveloF3 | This paper | N/A |
| pCS2-GFP-myc-XveloF4 | This paper | N/A |
| pCS2-myc-mCherry | This paper | N/A |
| pCS2-RFP-HYLS | Gift from Brian Mitchell | N/A |
| pCS2-RFP-Sas6 | Gift from Brian Mitchell | N/A |
| pCS2-myc-Sas6 | Gift from Brian Mitchell | N/A |
| pCS2-myc-xDZIP1 | Jin et al.[73] | N/A |
| pCS2-mCherry-myc-xDZIP | Jin et al.[73] | N/A |
| pCS2-mCherry-Cenexin | Addgene | Plasmid #186435 |
| pEGFP-Cep164 | Addgene | Plasmid #41149 |
| pEGFP-C3-PLK4-3xFLAG | Addgene | Plasmid #69837 |
| pCS2-Dnd1-GFP | Aguero et al.[96] | N/A |
| pCS2-Pgat-GFP | Aguero et al.[96] | N/A |
| pCS2-Nanos-ORF-GFP-SV40 | Aguero et al.[96] | N/A |
| pCS2-Dazl-GFP | Aguero et al.[96] | N/A |
| pGEX-6p1-GST-F1 | This paper | N/A |
| pGEX-6p3-GST-F3 | This paper | N/A |
| pGEX-6p3-GST-F4 | This paper | N/A |
| pGEX-6p1-GST-GFP | This paper | N/A |
| pCS2-HA | Addgene | Plasmid #16330 |
| Software and algorithms | | |
| ImageJ | Schneider et al.[97] | https://imagej.net/ij/index.html |
| Adobe Illustrator | Adobe Illustrator | https://adobe.com/products/illustrator |
| GraphPad Prism | GraphPad | https://www.graphpad.com/ |
| BioRender | Biorender | https://www.biorender.com |

## EXPERIMENTAL MODEL AND STUDY PARTICIPANT DETAILS

### Cell culture and transfection

HEK293T cells and HeLa cells were maintained in Dulbecco's Modified Eagle Media (DMEM) supplemented with 10% Fetal Bovine Serum (FBS) and 50IU/ml penicillin-streptomycin. Transfections were carried out using Polyethylenimine (PEI). 100 μM (2.5 mg/ml) PEI was dissolved in 1X HBS (150mM NaCl and 20mM HEPES-NaOH, pH 7.4). From a 2.5mg/ml stock, 3μl PEI was used for every 1μg of plasmid transfected. Opti-MEM™ media mixed with PEI was added to Opti-MEM™ media mixed with the plasmids. After 20min incubation at room temperature, the mix was added dropwise to the cells prepared for transfection. The media was replaced with fresh pre-warmed DMEM media 4h post-transfection.

## METHOD DETAILS

### Cellular fractionation

HEK293T cells were transfected with Xvelo (0.5μg) in addition to either a control plasmid (pCS2-HA) or centrosome components (0.5μg). For F3 and F4, due to low expression, 0.75μg was used instead. 24h post-transfection, the cells were washed with cold PBS, followed by lysis on ice using 1% NP40 lysis buffer (50mM Tris pH 7.6, 125mM NaCl, 1mM EDTA, 1% NP40%, and Protease inhibitor cocktail) for 10 minutes. Collected lysates were subjected to centrifugation at 13,000 rpm for 5min on a tabletop centrifuge, followed by separation of supernatant and pellet fractions. Samples were further processed with SDS Sample buffer for western blot.

### Western Blot

Western blot samples were boiled for 5min at 95°C, left on ice for 2min, followed by a quick spin. The supernatants were loaded on SDS-PAGE gel. After the electrophoresis, proteins were transferred to a PVDF membrane. For blocking, PVDF membranes were incubated with 5% nonfat dry milk (in 1XTBST: Tris-buffer saline + 0.1% Tween 20). This was followed by overnight incubation with primary antibody, and secondary antibody incubation the next day. After washing with 1xTBST extensively, the membranes were developed using ECL™ Prime Western Blotting Detection Reagent. For quantification of western blots, the HSC70 (or myc

control in Figures 1D and 5C) controls were used for normalization. The normalized intensity of all bands was compared to the control Sup intensity. Statistical analysis was performed using two-way ANOVA, followed by Fisher's LSD post hoc test using GraphPad Prism.

### Mito-tracker and ER tracker staining

HEK293T or HeLa cells were seeded on glass-bottom dish and transfected the next day with 0.5μg Xvelo. One day post-transfection, the cells were incubated in Fluorobrite™ DMEM with 100nM mito-tracker or 1000nM ER tracker for 30min, along with Hoechst to visualize the nuclei. Xvelo aggregates and mitochondria or ER were then imaged using the Nikon A1R confocal microscope.

### Fluorescence recovery after photo bleaching (FRAP)

HEK293T cells were seeded on a glass-bottom dish and transfected the next day with 0.5μg Xvelo. One day post-transfection, DMEM was replaced with pre-warmed Fluorobrite™ DMEM. A Nikon A1R confocal microscope was utilized to perform the FRAP experiment. An ROI was selected on the Xvelo aggregates that were subject to photobleaching using lasers with 50% power. The recovery of Fluorescence after bleaching was monitored every 30sec for about 10min. ImageJ was used for further analysis involving measurement of fluorescent intensity over time in the bleached region and normalized to an unbleached region of the same size on the aggregate.

### Immunostaining

HEK293T or HeLa cells were seeded on coverslips and transfected with mCherry-Xvelo the next day. 24h post-transfection, the cells were fixed with 4% PFA for 20min at room temperature. The coverslips were washed 4 times with 1X PBS, followed by 10min permeabilization with PBST (1X PBS with 0.1% Triton X-100). Coverslips were then incubated with blocking buffer (containing 1% BSA + 5% Normal Goat Serum) for one hour. After blocking, the cells were incubated overnight at 4°C with primary antibody (rabbit anti-B56ε). The following day, after washing with PBS 4 times, the cells were incubated with secondary antibody (goat anti-rabbit-488) for 1h. The coverslips were washed with PBS 4 times, incubated with DAPI (1:1000) for 5min, and then mounted on slides for imaging.

### Lentiviral knockdown

HEK293T cells were transfected with viral packaging vectors pAX2 and pMD2, along with a non-target scrambled control shRNA or shRNAs against Sas6, Cenexin (ODF2) and DZIP1. All shRNA vectors were purchased from Sigma Aldrich. 24h post-transfection, the viral soup was collected every 12h for 3 days and stored at 4°C till the cells were ready to be infected. Meanwhile, some HEK293T cells were transfected with Xvelo (pCS2-GFP-Flag-Xvelo) and a control plasmid (pCS2-myc-mCherry). Two days after transfection, the transfected cells were infected with either a non-target control virus or viral soup for knockdown of centrosome components (Sas6, Cenexin and/or DZIP1). For knockdown of multiple centrosome components, the cells were infected with virus for shSas6, shCenexin, and shDZIP1 sequentially for 24h each. Puromycin selection was allowed overnight using 10μg/ml Puromycin. To validate the knockdown, RNA from cells was extracted using TRIzol reagent. This was followed by cDNA synthesis using M-MLV Reverse Transcriptase enzyme, and real-time PCR using 2X SYBR Green qPCR Master Mix. The Applied Biosystems QuantStudio 3 Real-Time PCR system was utilized to obtain Ct values. The primers for qPCR are listed under supplemental information (Table S1).

### GST pulldown

pGEX-6p1-GST-F1, pGEX-6p3-GST-F3, pGEX-6p3-GST-F4 and pGEX-6p1-GST-GFP were expressed in BL21 cells, followed by induction with 1mM IPTG for 4h at 30°C. Following sonication, the cleared lysates were incubated with Glutathione Sepharose beads for 3h at 4°C. After thoroughly washing the beads with lysis buffer (300g for 30s each wash), we estimated the amount of protein by Coomassie Brilliant Blue staining. For the pull-down experiments, cleared lysates were obtained from HEK293T cells that were previously transfected with Sas6, xDZIP1, or Cenexin. After saving the 'Input', the rest of the lysates were incubated overnight at 4°C with roughly similar amounts of GFP/F1/F3/F4 protein-coated beads. The next day, the beads were washed 4 times with lysis buffer (300g for 30sec each), 1X SDS Sample buffer was added to the beads, and samples were processed for western blot analysis.

## QUANTIFICATION AND STATISTICAL ANALYSIS

All information regarding quantification and statistical analysis is provided in either figure legends or method details. All image and statistical analysis were done using ImageJ[97] and GraphPad Prism respectively.